*Acta Mineralogica-Petrographica, Szeged 2008, Vol. **48**, pp. 17-31.*

ACTA Mineralogica Petrographica

# SHOCK METAMORPHISM AT TERRESTRIAL IMPACT STRUCTURES: MINERALOGICAL AND GEOLOGICAL CONSEQUENCES

ARNOLD GUCSIK

Max Planck Institute for Chemistry, Department of Geochemistry, Joh.-J.-Becherweg 27., D-55128, Mainz, Germany.
e-mail: gucsik@mpch-mainz.mpg.de

**ABSTRACT**

The impact cratering as a leading process in the formation of the planetary bodies and surfaces and their geological as well as mineralogical consequences have been summarized in this review article, which is based on PhD. thesis of Arnold Gucsik at Univeristy of Vienna. The purpose of this study is to provide the most important lithological and shock diagnostic features of shock metamorphism accompanied with terrestrial impact structures. The first section of this study gives a brief summary of the formation mechanism and stages of an impact structure as well as a short description of basics of the sock wave physics of an impact event. The next section deals with the types of terrestrial impact structures. The lithological shock-metamorphic indicators and diagnostic shock features in the target rocks are mentioned in the following sections.

***Key words:*** shock metamorphism, impact crater, shock wave, impact-derived glasses, shock-induced microdeformations

## INTRODUCTION

Shock metamorphism is the sum of irreversible chemical, mineralogical and physical changes in the target materials that occur during the hypervelocity impact event (Melosh 1989). The following chapters have been summarized from reviews by French and Short (1968), Sharpton and Grieve (1990), Stöffler and Langenhorst (1994), Grieve et al. (1996), Koeberl (1997) and French (1998). When an extraterrestrial projectile (comet or asteroid) hits target rocks of a planetary surface, geologic materials are subjected to shock pressures above their Hugoniot Elastic Limit (HEL), which is on the order of 5 to 10 Gigapascals (GPa) (Sharpton and Grieve 1990). Shock metamorphism provides evidence for conditions associated with impact cratering (e.g., French and Short 1968, Stöffler and Langenhorst 1994, Grieve et al. 1996, Koeberl 1997, French 1998 and references therein) including the high pressures, temperatures, and strain rates (106-108 s-1), which lead to characteristic structural and phase changes in minerals. Figure 1 shows a comparative pressure-temperature diagram of endogenic metamorphism and shock metamorphism (Koeberl 1997). The most characteristic products of shock metamorphism, as well as the associated diagnostic features are listed in Tables 1 and 2. These diagnostic shock features are the most important criterion to evaluate the impact origin of a crater, in particular when characteristic features of progressive shock metamorphism, as listed in Tables 1 and 2, are found.

Large impact events differ in many ways from endogenic processes such as volcanic explosions, earthquakes, and plate tectonics (French 1998):

- There have been no historical records or examples of large meteorite impacts.
- The impact energy is limited only by the mass and velocity of the projectile and concentrated within a fraction of time compared to the hundreds or thousands of years through volcanism, earthquakes, tectonic processes, and heat flow.
- The energy is released in an impact event shattering, deforming, melting, and even vaporising large volumes of target rock in a fraction of seconds.
- Large impact events cause biological extinctions, because their impact energy is released near the surface and directly into the biosphere.
- Unique deformation effects occurred as changes in minerals such as mineral deformations and melting under the extreme high pressure and temperature (e.g., the shock pressure is approximately 60 GPa and post-shock temperature is about 2000°C).

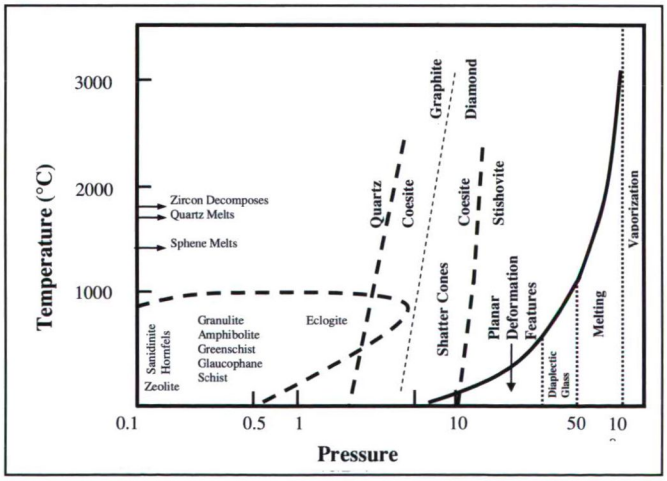


***Fig. 1.*** Conditions of endogenic metamorphism and shock metamorphism in the pressure-temperature fields. This comparison diagram exhibits the onset pressures of various irreversible structural changes in the rocks due to shock metamorphism and the relationship between pressure and post-shock temperature for shock metamorphism of granitic rocks (after Koeberl 1997, his Fig. 2).

***Table 1.*** Shock pressures and effects (from Stöffler and Langenhorst, 1994; French, 1998).

| Approximate Shock Pressure (GPa) | Estimated Post Shock Temperature (°C) | Effects |
|---|---|---|
| 2-6 | <100 | Rock fracturing; breccia formation; Shatter cones |
| 5-7 | 100 | Mineral fracturing: (0001) and $\{10\bar{1}\,0\}$ in quartz |
| 8-10 | 100 | Basal Brazil twins (0001) |
| 10 | 100 | |
| | | Quartz with PDFs $\{10\bar{1}\,3\}$ |
| 12-15 | 150 | Quartz → stishovite |
| 13 | 150 | Graphite → diamond |
| 20 | 170 | |
| | | Quartz with PDFs $\{10\bar{1}\,2\}$, etc. |
| | | Quartz, feldspar with reduced refractive indices, lowered birefringence |
| >30 | 275 | Quartz → coesite |
| 35 | 300 | |
| | | Diaplectic quartz, feldspar glasses |
| 45 | 900 | Normal (melted) feldspar (vesiculated) |
| 60 | >1500 | Rock glasses, crystallised melt rocks (quenched from liquids) |
| 80-100 | >2500 | Rock glasses (condensed from vapor) |

*For dense nonporous rocks. For porous rocks (e.g., sandstones), postshock temperatures = 700°C (P = 10 GPa) and 1560°C (P = 20 GPa).

***Table 2.*** Characteristics and formation pressures of various shock deformation features.

| Pressure (GPa) | Features | Target characteristics | Feature characteristics |
|---|---|---|---|
| 2-30 | Shatter cones | Best developed in homogeneous, fine-grained, massive rocks, both sedimentary and crystalline. | Conical fracture surfaces with subordinate striations radiating from a focal point. |
| 5-45 | Planar fractures (PF) and planar deformation features (PDFs) | Highest abundance in crystalline rocks; found in many rock- forming minerals; e.g., quartz, feldspar, olivine, and zircon | PDFs: Sets of extremely straight, sharply defined parallel lamellae; occur often in multiple sets with specific crystallographic orientations. |
| 30-40 | Diaplectic glass | Most important in quartz and feldspar (e.g., maskelynite from plagioclase). | Isotropization through solid-state transformationunder preservation of crystal habit as well as primary defects and sometimes planar features. Index of refraction lower than in crystal but higher than in fusion glass. |
| 15-50 | High-pressure Polymorphs | Quartz polymorphs (coesite, stishovite) most common, but also ringwoodite from olivine, jadeite from plagioclase, and majorite from pyroxene. | Recognisable by crystal parameters, confirmed usually with XRD or NMR; abundance influenced by post-shock temperature and shock duration; Stishovite is temperature liable. |
| >35 | Impact diamond | From carbon (graphite) present in target rocks; rare | Cubic and hexagonal form; usually very small but occasionally up to millimetre-size; inherit graphite crystal shape |
| 45->70 | Mineral melts | Rock-forming minerals (e.g., lechatelierite from quartz) | Contrary to diaplectic glass, liquid-state transformation of a mineral into glass. |
| >60 | Rock melt | Best developed in massive silicate rocks. Occur as individual melt bodies (millimetre to meter size) or as coherent melt sheets, up to >1000 km3. | Either glassy (fusion glasses) or crystalline; of macroscopically homogeneous, but microscopically often heterogeneous composition. Large melt sheets may be medium to coarse-grained, and resemble endogenetic igneous rocks. |

GPa = Gigapascals; XRD = X-ray diffraction; NMR = nuclear magnetic resonance; PDFs = planar deformation features (after Koeberl, 1997, his Table 1).

## IMPACT CRATERING MECHANICS

The impact cratering process is commonly divided into the contact and compression, excavation, and modification stages (Gault et al. 1968, Melosh 1989, 1992). During the compression stage, structural modifications and phase changes occurred in the target rocks. The morphology of a crater is developed in the excavation and modification stages (Fig. 2).

*Contact and compression stage*

During the contact and compression stage, the projectile or impacting object first hits the planet's surface (the target) and transfers its energy and momentum to the underlying rocks. The projectile traveling at a few kilometers per second produces large specific kinetic energy ($E=½\ mv^2$, m = mass, v = velocity) (Melosh 1992). For instance, a stony meteorite of only 6 m diameter, colliding with the Earth at 20 km/s, releases as much energy [8.3 x 1023 Joules (J) or 20,000 tons (20 kT) of TNT] as an atomic bomb (French 1998).

This stage lasts only a bit longer than the time required for the impacting object to travel its own diameter,

$$t_{cc}= L/v_i, \quad (1)$$

where $t_{cc}$ is the duration of contact and compression, L the projectile diameter, and $v_i$ the impact velocity.

The shock wave in the projectile reaches its back (or top) surface in contact and compression stage. Simultaneously, the pressure is released as the surface of the compressed projectile expands upward (wave of pressure relief propagates back downward toward the projectile-target interface). During the irreversible compression process, the projectile has been compressed to high pressure (hundreds of gigapascals) producing liquid or gaseous state due to heat deposited in the projectile (Melosh 1992).

Very high velocity jets of highly shocked material are formed, where strongly compressed material is close to a free surface. The jet velocity depends on the angle between the converging surface of the projectile and the target, but may exceed the impact velocity by factors as large as five (Melosh 1992).

*Hugoniot Elastic Limit (HEL)*

The projectile hits the target, generating strong shock waves, which leads to compression of the target rocks at pressures far above a material parameter called the Hugoniot elastic limit (Melosh 1989). The Hugoniot Elastic Limit (HEL) describes the maximum stress in an elastic wave that a material can be subjected to without permanent deformation (Melosh 1989). The value of the HEL is about 5-10 GPa for most minerals and whole rocks. The only known natural process that generates these high shock pressures exceeding the HELs is hypervelocity impact. The strength of the shock waves can be demonstrated or measured from the Hugoniot equations, relating quantities in front of the shock wave (subscript 0) to quantities behind the shock wave (Melosh 1989)

$$\rho(U-\mu_p) = \rho_0 U \quad (2)$$

$$P-P_0 = \rho_0 \mu_p U \quad (3)$$

$$E-E_0 = ½(P + P_0)(1/\rho_0-1/\rho) \quad (4)$$

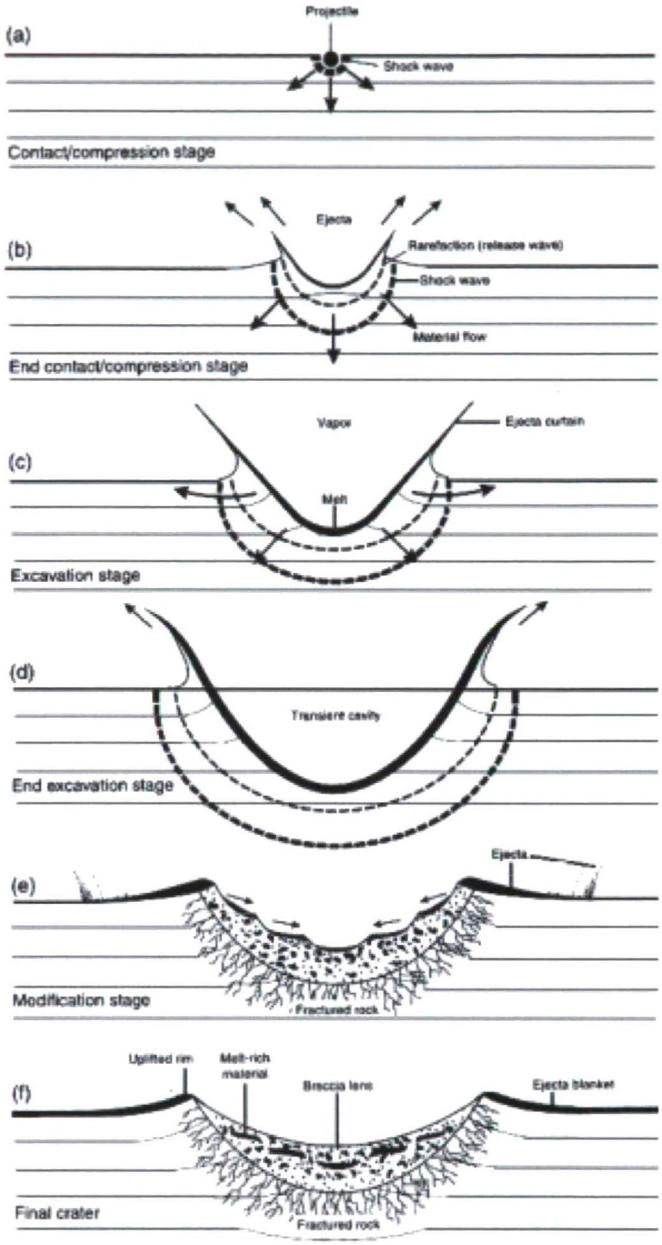


***Fig. 2.*** Schematic diagram of the stages of the formation of a simple impact crater (from French, 1998; Fig.3.3).

where P is pressure, ρ density, $\mu_p$ particle velocity after the shock, U the shock velocity, and E energy per unit mass. These three equations are equivalent to the conservation of mass, momentum, and energy, respectively, across the shock front. The Hugoniot equations must be supplemented by a fourth equation, the equation of state, that relates the pressure to the density and internal energy in each material,

$$P = P(\rho, E) \quad (5)$$

Alternatively, a relation between shock velocity and particle velocity may be specified,

$$U = U(\mu_p) \quad (6)$$

As this relation is frequently linear, it often provides the most convenient equation of state in impact processes. Thus, we can write:

$$U = c + S\mu_p \quad (7)$$

where c and S are empirical constants. Table 3 lists the measured values of c and S for a variety of materials. These equations can be used to compute the maximum pressure, particle velocity, shock velocity, etc. in an impact (Melosh 1992). A Hugoniot equation of state curve is a shock wave equation of state data, which are plotted on a P-V plane (Fig. 3). It defines the locus of all shock states achievable in any material by shock waves of variable intensity, e.g., by various impact velocities of a projectile (Melosh 1989, Koeberl 1997).

Temperatures in the shocked states can be determined by integrating the following equation because of the internal energy, which is related to temperature and volume through an equation of state (Martinez et al. 1995, Martinez and Agrinier 1998):

$$\frac{dt}{dV} = -T\left(\frac{\gamma}{V}\right) + \left[\frac{dP}{dV}(V_0 - V) + (P_0 - P)\right]\frac{1}{2C_v} \quad (8)$$

where V0 and P0 are initial volume and pressure.

Models of specific heat Cv and Grüneisen parameters γ (which are quantities that are relatively constant by the product of three times the coefficient of linear expansion divided by the product the compressibility with the specific heat per unit volume) at high temperature and compression are therefore required for calculating shock temperatures (Melosh 1989, Martinez and Agrinier 1998).

Post-shock temperatures in the material can be related to temperatures in the shocked state using

$$\frac{dT}{dV} = -T\left(\frac{\gamma}{V}\right) \quad (9)$$

which is the adiabatic part of the Hugoniot equation and represents the adiabatic decompression from the shock state to the final surface-pressure state (Melosh 1989, Martinez and Agrinier 1998).

*Excavation stage*

As Figure 4 shows, the expanding shock waves open the actual impact crater during the excavation stage (Melosh 1989, Grieve 1991). The transient cavity is a freshly opened bowl-shaped crater and surrounded by an ejecta curtain that develops is several orders of magnitude larger than the diameter of the projectile.

At the high pressures and post-shock temperatures the rocks may melt or even vaporise upon release. The lower pressures cause pervasive fracturing and planar deformation elements in individual crystals and produce characteristic cone-in-cone fractures called shatter cones. The target material strength and gravity become important near the end of excavation. This stage ends much longer than the contact and compression stage, requiring seconds or minutes to reach completion, depending upon the several factors as follows: crater size, direction of the impact, impact velocities, presence of a water table or layers of different strength, rock structure, joints, or initial topography in the target (Melosh 1992).

*Modification stage*

The modification stage begins when the transient crater collapses under gravity, and elastic rebound of the underlying, compressed rock layers may also play a role. It was suggested from volume conservation that the crater collapse appears almost immediately after formation of the transient crater, which produces an increase of the original diameter of the crater by about 15%. During modification, loose debris slides down the steep interior walls of small craters, pooling on the floor of the final bowl-shaped depression (Melosh 1992). The normal geologic processes of gradation, isostatic adjustment, infilling by lavas, sediments, etc. on geologic time scales may eventually result in obscuration or even total obliteration of the crater (Melosh 1992).

***Table 3.*** Linear shock-particle velocity equation of state parameters (from Melosh, 1989, 1992).

| Material | $\rho_0$ (g/cm$^3$) | c (km/s) | S |
|---|---|---|---|
| Aluminium | 2.750 | 5.30 | 1.37 |
| Basalt | 2.860 | 2.60 | 1.62 |
| Calcite (carbonate) | 2.670 | 3.80 | 1.42 |
| Coconino sandstone | 2.000 | 1.50 | 1.43 |
| Diabase | 3.000 | 4.48 | 1.19 |
| Dry sand | 1.600 | 1.70 | 1.31 |
| Granite | 2.630 | 3.68 | 1.24 |
| Iron | 7.680 | 3.80 | 1.58 |
| Permafrost (water saturated) | 1.960 | 2.51 | 1.29 |
| Serpentinite | 2.800 | 2.73 | 1.76 |
| Water (25°C) | 0.998 | 2.393 | 1.33 |
| Water ice (-15°C) | 0.915 | 1.317 | 1.53 |

$\rho_0$ is the density of material in front of shock wave, c and S are empirical constants.

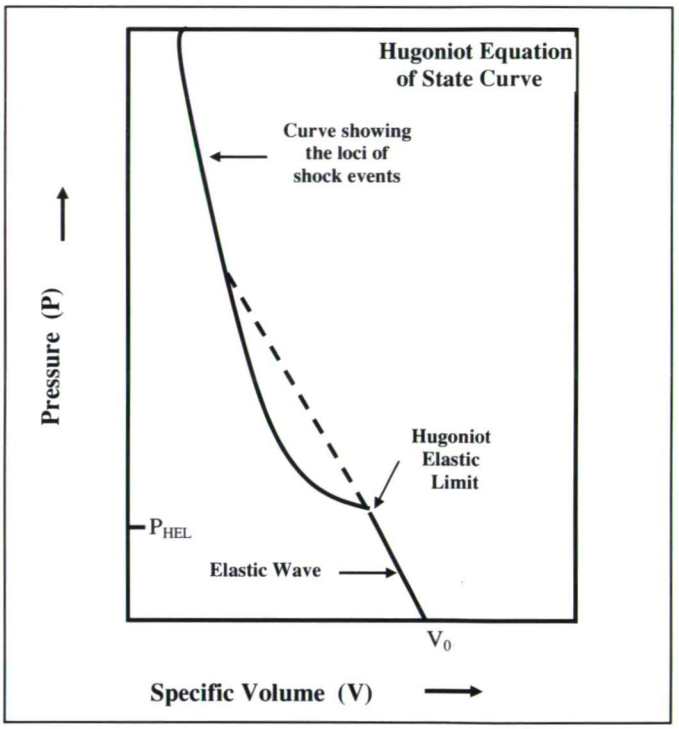


***Fig. 3.*** The Hugoniot equation state curve does not represent a continuum of states as in thermodynamic diagrams, but the loci of individual shock compression events. The yielding of the material at the Hugoniot Elastic Limit is indicated (after Koeberl 1997, his Fig. 1).

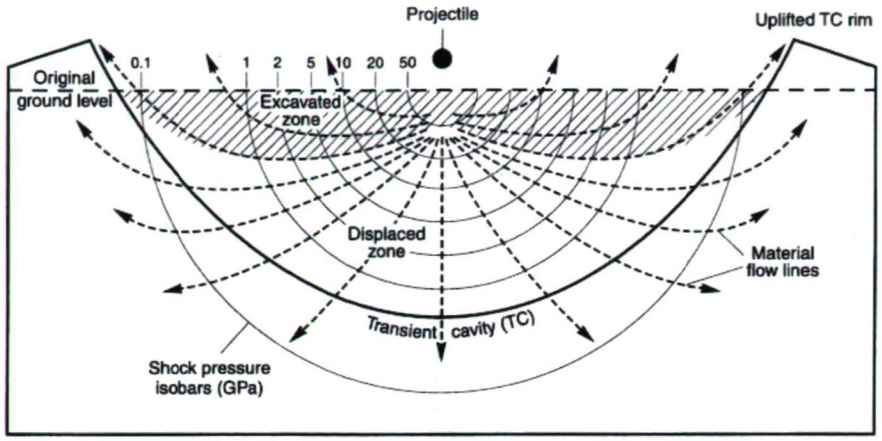


***Fig. 4.*** Theoretical cross section showing development of the transient crater during the excavation stage immediately after the contact/compression stage. The hemispherical isobars around the impact point are original peak shock pressures in Gigapascals (GPa). The subsequent rarefaction wave produces an outward excavation flow (dashed arrows) that opens up the transient crater. In the upper part of this region (excavated zone; ruled area), target material is fractured, excavated, and ejected beyond the transient rim. In the lower region (displaced zone), target material is driven downward and outward, more or less coherently, and thus does not reach the surface (from French 1998, his Fig.3.4).

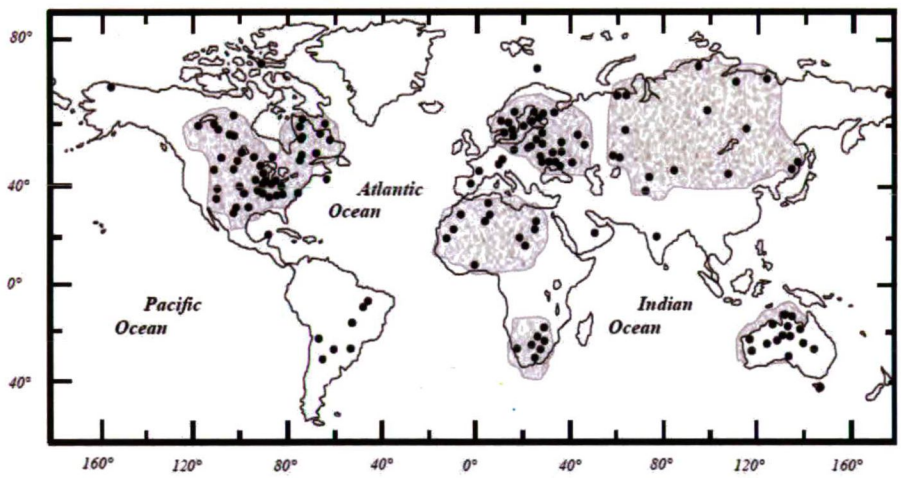


***Fig. 5.*** Distribution of currently (2009) known impact structures on Earth. The confirmed impact craters are concentrated mainly to the cratonic areas (as indicated by grey regions) of continents. So far no impact structures on the ocean floor have been identified (data from www.unb.ca/passc/Impact Database).

***Fig. 6.*** A young, well-known and well-preserved simple impact crater (1.2 km in diameter): Barringer Meteor Crater (Arizona, USA). This crater was formed about 50.000 years ago, when an iron meteorite approximately 30 m across struck the horizontal sediments of northern Arizona's Colorado Plateau. The photo, looking northwest, shows the uplifted rim (photo by the author).

## TYPES OF IMPACT CRATERS

The Earth Impact Database is a resource that has been assembled since 1985 by researchers at the Geological Survey of Canada (a division of Natural Resources, Canada). It has now been transferred to the Planetary and Space Science Centre at the University of New Brunswick, Department of Geology. Here, 175 impact structures (2009) were registered on the webpage: www.unb.ca/passc/ImpactDatabase/. These confirmed terrestrial impact craters (Fig. 5) have two basic morphological forms: simple and complex. The two forms differ only in the diameter range at which the transition from one form to another takes place. On the Earth, simple craters occur up to a diameter of 4 km in crystalline and 2 km in sedimentary target rocks (Dence 1972). Terrestrial craters with a diameter greater than 4 km show a complex form. Depending on their size, complex craters may be further subdivided into peak ring crater and multiring basins.

### *Simple Craters*

Simple craters are the smallest impact structures and occur as bowl-shaped depressions (French 1998). These craters can be characterized by a structurally upraised and fractured rim area (e.g., Barringer Crater, Arizona, USA) (Fig. 6). The sizes of these craters are up to 2 km (sedimentary target rocks) to about 4 km in diameter (crystalline target rocks) on Earth, depending on the strength of the target rocks (Dence 1972, Melosh 1992). The interior of the crater has a smoothly sloping parabolic profile and its rim-to-floor depth is about one-fifth of its rim-to-rim diameter. The surrounding plain is blanketed with a mixture of ejecta (proximal ejecta) and debris scoured from the pre-existing surface for a distance of about one crater diameter from the rim (Melosh 1992). The floor of simple craters is underlain by a lens of broken rock, breccia, which slid down the inner walls of the crater shortly following excavation. This breccia typically includes representatives from all the formations intersected by the crater and may contain layers of melted or highly shocked rocks (Fig. 7).

### *Complex craters*

The complex craters have flat interior floors or internal rings instead

of central peaks and formed with diameters larger than 4 km on Earth (depending on the target lithology). These craters are believed to have formed by collapse of an initially bowl-shaped transient crater, and because of this more complicated structure they are known as complex craters (Melosh 1992). The floors of complex craters are covered by melted and highly shocked debris. The surfaces of the terrace blocks tilt outward into the crater walls, and melt pools are also common in the depressions thus formed (Fig. 8). The central peaks consist of material that is pushed upward from the deepest levels excavated by the crater. Complex craters are generally shallower than simple craters of equal size and their depth increases slowly with increasing crater diameter. Rim height also increases rather slowly with increasing diameter because much of the original rim slides into the crater bowl as the wall collapses (Melosh 1992). The amount of structural uplift (SU) at complex craters can be measured, where the subsurface stratigraphy is known (Fig. 8). The relationship is:

$$SU=0.06D^{1.1} \qquad (10)$$

where SU is the amount of stratigraphic uplift undergone by the deepest lithology now exposed at the surface in the center and D is the diameter of the crater (Grieve 1991). The uplifted area may consist of parts of the upper crust at the larger complex craters (e.g., Siljan, SU=4 km; Manicouagan, SU=9.5 km). The ejecta blankets of complex craters show some similarities to those of simple craters. However, the hummocky texture characteristics of simple craters are replaced by more radial troughs and ridges as size increases (Melosh 1992).

*Submarine impact structures*

Only a few confirmed submarine impact craters are known, including: Montagnais, located offshore of Nova Scotia, Canada (50.5 Ma, D=45 km), Tvären, Sweden (455 Ma, D=2 km), Mjølnir in the Barents Sea, north of Norway (Jurassic, D=40 km), and Chesapeake Bay offshore of the Atlantic coast of Virginia, USA (35 Ma, D=90 km). The half of the Chicxulub multiring impact basin is

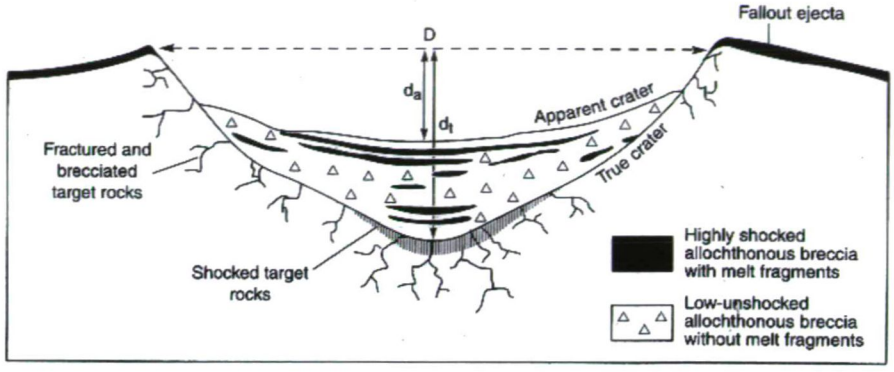


***Fig. 7.*** Schematic cross section of a simple impact structure, showing the locations of impactite types. Fractured and brecciated target rocks lie below the true crater floor without distinctive shock effects. Only the shocked target rocks as a small zone (fine vertical ruling) contain shock metamorphic effects in the center of the structure. The fallout ejecta overlies the uplifted crater rim and surrounds the crater, which is easily eroded and is presented only in the youngest and best-preserved structures. D= final crater diameter; dt= true depth of the final crater; da= apparent depth of the crater (from French 1998, his Fig.3.7).

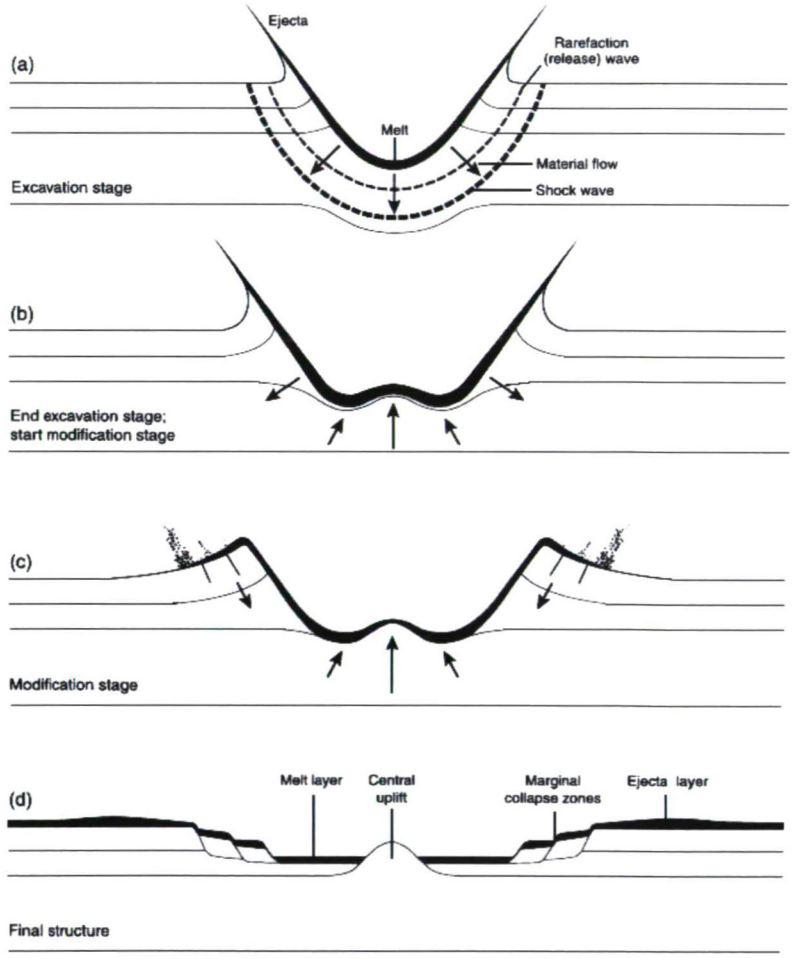


***Fig. 8.*** Stages of progressive development of a large, complex impact structure in a horizontal layered target: (a) formation of a large transient crater in the excavation stage; (b) initial development of central uplift during the modification stage; (c) start of peripheral collapse in the modification stage; (d) final structure showing a central uplifted area, which is surrounded by a relatively flat plain and by a terraced rim produced by inward movement along stepped normal faults. The central uplift is surrounded by an annular deposit of allogenic breccias and impact melt (black). An ejecta layer (stippled) covers the target rocks around the structure. (from French, 1998; his Fig.3.10).

buried by under roughly 1 km of Cenozoic sediments, which is located at the tip of the Yucatan Peninsula. The Kara Sea in Russia shows relics of a twin impact structure (71 Ma), Kara and Ust-Kara craters. The evidence for a Late Pliocene impact are described such as occurrence of microtektites and an iridium anomaly in abyssal sediments in an area of about 300 000 $km^2$ in the South Pacific (Eltanin Sea Mt.). However, the small-sized projectile (D= 0.5 km) probably did not reach the ocean floor (at a depth of ca. 5000 m). Craters on oceanic crust are unknown to date, reflecting not only the young mean age of the oceanic crust, but also our relatively poor knowledge of two thirds of the Earth's solid surface (Deutsch 1998).

## LITHOLOGICAL INDICATORS OF IMPACT STRUCTURES

An impact event is a surface process that produces circular, shallow, rootless structures in contrast to volcanic processes (French 1998). The lithological indicators for an impact structure may be a layer of fragmental breccia, which is found as crater filling or overlying a possibly raised, partially brecciated, and up- or over-turned rim (Koeberl 1997).

### *Breccia types at impact structures*

The impact-derived breccias contain shocked minerals, impact melts, and impact glasses in an impact crater (Stöffler and Grieve 1994, Koeberl 1997). The monomict and polymict breccias that formed during impact processes could be divided into three main types: (1) cataclastic (fragmental breccias), (2) suevitic (fragmental with a melt fragment component) breccias (Fig. 9), or (3) impact melt (melt breccia - i.e., melt in the matrix with a clastic component) breccias. The breccias can be allochthonous or autochthonous. Additionally, the basement rocks contain dikes of injected or locally formed fragmental or pseudotachylitic breccias (Reimold 1995). Whether all these breccia types are actually present at an impact crater depends on factors including the size of the crater, the composition of the target area (e.g., Kieffer and Simonds 1980), and the level of erosion (see Roddy et al. 1977, Hörz 1982, Grieve 1987 and references therein).

### *Complete melting*

The target rocks undergo complete (bulk) melting to form impact melts at pressures in excess of about 60 GPa. The resulting melts are deposited as splash-form glass particles and "bombs" in suevitic breccias or as coherent impact melt body. The presence of inclusions of minerals, such as lechatelierite (monomineralic quartz melt that forms from pure quartz at temperatures of 1700°C), or baddeleyite (thermal decomposition product of zircon forming at a temperature of at least 1680°C), is associated with very high temperatures. Lechatelierite as a good indicator of meteorite impact origin is not found in any other natural rock, except in fulgurites, which form by fusion of soil or sand when lightning hits the ground (Stöffler and Langenhorst 1994, and references therein).

### *Impact glasses*

Impact glasses are more commonly found at relatively young impact craters rather than at old impact structures, because glass is not stable over geological times. Such

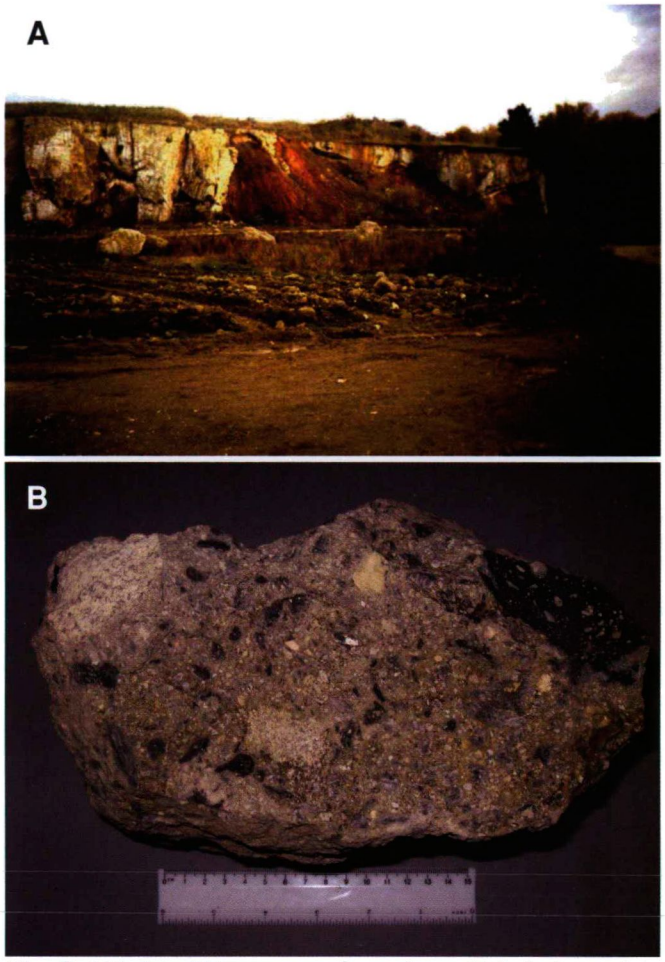


***Fig. 9.*** (A) Aumühle quarry of suevite, which is located in the northwest of the Ries impact structure (Germany). This image shows a dark Jurassic clay and red clay and sandstones of the Keuperian. (B) Suevite: the elongated, grey parts of suevite are impact glasses (photos by author).

impact-derived glasses have chemical and isotopic compositions that are similar to those of the target rocks. The similarities in chemical and isotopic composition between impactites and crater target rocks have been employed in several source crater investigations (e.g., French et al. 1970, Blum et al. 1993, Meisel et al. 1995). Impact glasses have much lower water contents (about 0.001-0.05 weight %) than volcanic or other natural glasses (Koeberl 1992a). These impact melts and glasses are useful for the dating of an impact structure using K-Ar, $^{40}Ar$-$^{39}Ar$, fission track, Rb-Sr, Sm-Nd, or U-Th-Pb isotope age-dating methods (Montanari and Koeberl 2000). The age that should be obtained for an impact event is different from that of volcanism because impact melts or glasses give a unique (local), much younger age as compared to the target rocks, which are usually old crustal rocks.

### *Tektites and microtektites*

The centimeter-sized tektites as chemically homogeneous glasses have been ejected from a few terrestrial impact structures and spread over thousands of kilometers. They found on land and have been subdivided into three groups: (a) normal or splash-form tektites, (b) aerodynamically shaped tektites, and (c) Muong Nong-type tektites (or layered

tektites). Tektites can be associated with smaller (≤1 mm) microtektekties (Montanari and Koeberl 2000).

Currently, on the basis of differences in location, age, and to some extent, the characteristics of tektites and microtektites, four strewn fields are known: (1) Australasian (0.78 Ma, source crater no yet identified); (2) Central European (15 Ma) from the Ries Crater, Germany; (3) Ivory Coast (1.07 Ma) from the Bosumtwi Crater, Ghana (Koeberl et al. 1997a); and (4) North American (35 Ma) from the Chesapeake Bay impact structure, USA (Koeberl et al. 1997a) (Fig. 10).

Tektites are formed as the product of melting and quenching of terrestrial rocks during hypervelocity impact on the Earth (see Montanari and Koeberl 2000, for a recent review). Their chemical and isotopic compositions are identical with those of the target rocks where the impact occurred:

- Typically high in silica composition (>65 weight %), but their chemical and isotopic compositions are not volcanic, but closer to those of shales and similar sedimentary rocks. Containing low water content (≤0.02 wt %), and their flow-banded structure includes particles and bands of lechatelierite (monomineralic quartz melt).
- A few tektites contain partly melted inclusions of shocked and unshocked mineral grains (quartz, apatite, zircon) as well as coesite (Glass and Barlow 1979).

The Aouelloul crater is situated at 20°15'N and 12°41'W in the Ardar region, Western Sahara Desert, Mauritania (e.g., Koeberl 1994). The fission track and K-Ar dating of the impact glass show that this crater was formed 3.1 ± 0.3 Ma ago (Fudali and Cressy 1976, Storzer and Wagner 1977). The crater has a rim to rim diameter of 390 meters is exposed in an area of Ordovician Oujeft quartzite and Zli sandstone (Koeberl et al. 1998). Aouelloul impact glasses contain lechatelierite and baddeleyite (El Goresy 1965, El Goresy et al. 1968), , as well as partly digested quartz and feldspar grains, have a low water content (Beran and Koeberl 1997), and abundant schlieren of different chemical composition (Koeberl 1994). The composition of the glass is similar to that of the sandstone in which the crater is exposed, but some siderophile elements are enriched in the glass (Koeberl and Auer 1991). Re-Os isotope studies of the target sandstone and the impact glass were performed and demonstrated the presence of a distinct extraterrestrial component in the glass (Koeberl et al. 1998).

Muong Nong-type tektites are a subgroup of tektites that are abundant in the Australasian strewn field, These tektites differ in some characteristics from "normal" tektites: (1) they have higher concentrations of volatile elements (e.g., Cl, Br, Zn, Cu, Pb); (2) they are chemically inhomogeneous on a millimeter scale; (3) they contain dark and light layers with different chemical composition; (4) they may contain relict mineral inclusions (e.g., zircon, chromite, rutile, quartz, monazite) (e.g., Glass 1972, Deloule et al. 2001); (5) they contain large and more abundant bubbles that may be ellipsoidal, showing glass flow; (6) they have a large and irregular sample size with no sign of ablation (cf. Koeberl 1992b).

Libyan Desert Glass (LDG) is a natural glass found in an area of about 3500 $km^2$ between linear sand dunes of the southwestern corner of the Great Sand Sea in western Egypt, near the Libyan border. This glass occurs as fragments of a broad range of sizes (from centimeter -to decimeter-sized irregular and strongly wind-eroded blocks) (Barrat et al. 1997). In terms of chemical composition, LDG is very silica-rich (approximately 98 wt% of $SiO_2$ content) and has low abundances of most major oxides. The age of LDG was determined by fission-track analysis giving ages ranging from 28.5±2.3 Ma to 29.4±0.5 Ma (plateau age) (e.g., Bigazzi and de Michele 1996; Horn et al. 1997). The origin of LDG has been the subject of much debate since it was discovered early in the 20th century. Many workers were of the opinion that LDG is an impact glass, but were deterred by the lack of a suitable impact crater. Most researchers have now accepted the geochemical and geological evidence for an impact origin of LDG (McHone et al. 2000). Evidence for an impact origin includes the presence of lechatelierite (Diemer 1997), baddeleyite (Storzer and Koeberl 1991, Rocchia et al. 1997), and the likely existence of an extraterrestrial component in the glass (e.g., Rocchia et al. 1997, Murali et al. 1997). Previous cathodoluminescence data by Piacenza (1997) were interpreted to show evidence for a granular structure and the presence of lechatelierite. Cathodoluminescence microphotographs were used by Cipriani et al. (2000) in the determination of a possible extraterrestrial body signature in LDG. They concluded that the luminescence of Libyan Desert Glass is intrinsic, not induced by particle damage as in the case of amorphous silica.

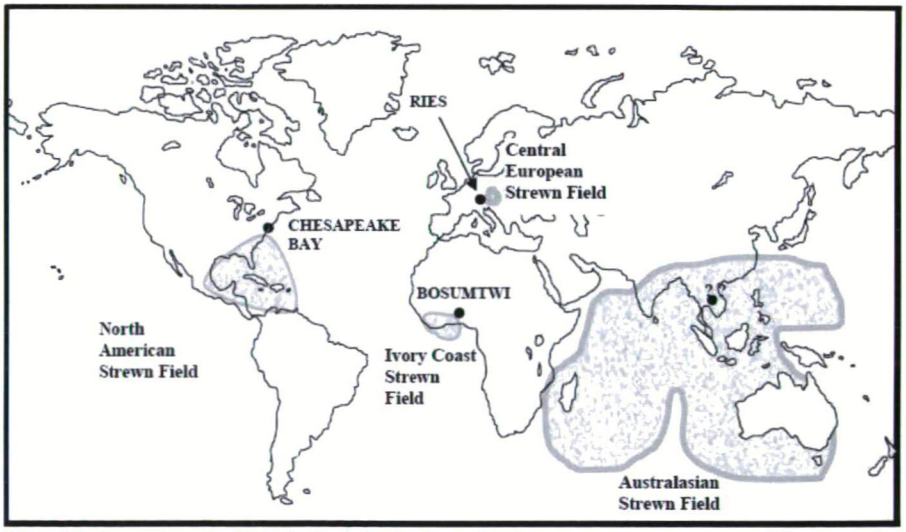


***Fig. 10.*** Location (solid circles) including the known source craters (Chesapeake Bay, Ries, and Bosumtwi craters) and extension of the four tektite strewn fields, which were classified by differences in location, age, and to some extent, the characteristics of tektites and microtektites on Earth (after Montanari and Koeberl 2000, their Fig. 2.4.1.1).

## DIAGNOSTIC SHOCK FEATURES IN IMPACT CRATERS

The best diagnostic indicators for shock metamorphism are features that can be studied easily by using the polarizing microscope. They include planar microdeformation features; optical mosaicism; changes in refractive index, birefringence and optical axis angle; isotropization; and phase changes (Stöffler 1972, 1974, Stöffler and Langenhorst 1994, Grieve et al. 1996, Koeberl 1997).

*Shatter cones*

Shatter cones (Fig. 11) are regarded as the only distinctive and unique shock deformation feature that develops on a macroscopic scale as hand specimen (Dietz 1968, French 1998). They are distinctive conical fractures produced in target rocks by shock waves of relatively low intensity, usually below the crater floor or in the central uplifts of large structures. They form in all kinds of target rocks subjected to the appropriate pressures, but they are most strikingly developed in fine-grained rocks, especially carbonates. Shatter cones can be distinguished from similar deformation features by the distinctive radiating striations ("horsetailing") along the cone surface, and by the fact that the cones originally point in the direction of the source of the shock wave, i.e., inward and upward. They develop in a large volume of target rock and have been widely used to identify terrestrial impact structure. Shatter cones are good diagnostic structural criteria that are easy to recognize and are found in many terrestrial impact structures.

The formation mechanism for shatter cones is poorly understood. The conical shapes might be related to the interactions of shock waves with point inhomogeneites in rocks, or interactions between the main compressive shock and rebound waves (Gash 1971). However, these models do not explain the dominant features of shatter cones such as characteristic striations, the "horse-tail" cone hierarchy, and the variety of complete cones. More recently, Shagy at al. (2002) have shown that the shatter cones are branched tensile fractures. Shatter-cone striations are the preserved tracks of fracture front waves. Their analysis of the striations shows that shatter cones develop only at extreme propagation velocities, between $0.9V_R$ and the maximal permitted velocity of $V_R$. The angles of the striations ($\alpha$), which are shown to increase systematically with the distance from the impact, reflect both the stresses and the energy flux driving the fracture at a given site, and may be used as a general tool to evaluate extreme local stresses in the field (Shagy et al. 2002).

***Fig. 11.*** Well-developed finely sculptured shatter cone, in fine-grained Ordovician limestone from the Charlevoix impact crater, Canada (photo by the author).

*Mosaicism*

The term mosaicism describes the internal fragmentation of a single crystal into a mosaic of slightly disoriented crystal domains. Mosaicism is a microscopic expression of shock metamorphism observed in a number of rock-forming minerals (see, e.g., Hörz and Quaide 1973) and appears as an irregular, mottled optical extinction pattern. This is distinctly different from the undulatory extinction that occurs in tectonically deformed quartz and, generally, accompanied in many minerals by indications of plastic deformation structures or deformation bands (Stöffler 1972). Mosaicism can be semi-quantitatively investigated by X-ray diffraction.

*Kink Bands*

Kink bands appear in sheet silicates, other sheet-like structures in shocked quartz and feldspar (Bunch 1968). They are not oriented parallel to rational crystallographic planes and display variable disorientation with respect to the host lattice compared to the deformation twins. Kink banding is considered as supporting evidence for the impact origin of

***Table 4.*** Characteristics of planar fractures and planar deformation features in quartz. Data from Stöffler and Langenhorst (1994).

| | |
|---|---|
| Nomenclature | 1. Planar fractures (PF)<br>2. Planar deformation features (PDF)<br>2.1. Nondecorated PDFs<br>2.2. Decorated PDFs |
| Crystallographic orientation | 1. PFs: usually parallel to $(00\bar{1}1)$ and $\{10\bar{1}1\}$<br>2. PDFs: usually parallel to $\{10\bar{1}3\}$,$\{10\bar{1}2\}$, $\{10\bar{1}1\}$, (0001), $\{11\bar{2}2\}$, $\{11\bar{2}1\}$, $\{10\bar{1}0\}$, $\{11\bar{2}0\}$, $\{21\bar{3}1\}$, $\{51\bar{6}1\}$, etc. |
| Optical microscope properties | Multiple sets of PFs or PDFs (up to 15 orientations per grain)<br>Thickness of PDFs: <2-3 μm<br>Spacing: >15 μm (PFs), 2-10 μm (PDFs) |
| TEM properties (PDFs) | Two types of primary lamellae are observed:<br>1. Amorphous lamellae with a thickness of about 30 nm (at pressures of <25 GPa) and about 200 nm (at pressures of >25 GPa)<br>2. Brazil twin lamellae parallel to (0001) |

a structure, but it cannot be used as a single diagnostic criterion, as it occurs also in metamorphic rocks.

*Planar microstructures*

Two types of planar microstructures are apparent in shocked minerals: planar fractures (PFs) and planar deformation features (PDFs). Their essential characteristics are summarized in Table 4. The PDFs occur as either non-decorated or decorated PDFs (Stöffler and Langenhorst 1994). Planar deformation features in rock-forming minerals (e.g., quartz, feldspar, or olivine) are generally accepted to provide diagnostic evidence for shock deformation (see, e.g., French and Short 1968, Stöffler and Langenhorst 1994, Grieve et al. 1996, French 1998, and references therein).

*Planar Fractures (PF)*

Planar fractures are parallel sets of multiple planar cracks or cleavages in quartz grains; they develop at the lowest pressures characteristic of shock waves (~5-8 GPa) (French, 1998). As French (1998) noted, they are parallel to rational crystallographic planes with low Miller indices, such as (0001) and $\{10\bar{1}1\}$. The fractures are typically 5-10 μm wide and spaced 15-20 μm or more apart in individual quartz grains. Similar cleavage occurs also rarely in quartz from non-impact settings, and therefore planar fractures cannot be used independently as a single criterion for meteorite impact. However, the development of intense, widespread, and closely spaced planar fractures are frequently accompanied in impact structures by other features clearly formed at higher shock pressures (French 1998, and references therein). Planar deformation features, together with the somewhat less specific planar fractures (PFs) (Fig. 12), are usually well developed in quartz (Stöffler and Langenhorst 1994).

*Planar Deformation Features (PDFs)*

PDFs in various minerals (especially in quartz) have long been known as evidence of impact-induced deformation. In contrast to planar fractures, PDFs are not open cracks. They occur as multiple sets of more closely spaced (typically 2-10 μm), narrow (typically <2-3 μm), parallel planar regions than planar fractures (Fig. 13). PDFs occur in planes corresponding to specific rational crystallographic orientations. The basal (0001) or c, $\{10\bar{1}3\}$ or ω, and $\{10\bar{1}2\}$ or π, orientations are the most common planes in quartz. In addition, PDFs often occur in more than one crystallographic orientation per grain. At pressures about ≥35 GPa, the distances between the planes decrease, and the PDFs become more closely spaced and more homogeneously distributed over the grain. Depending on the peak pressure, PDFs are observed in 2 to 10 (maximum 18) orientations per grain (Robertson et al. 1968, Stöffler 1972, Stöffler and Langenhorst 1994, Grieve et al. 1996, Koeberl 1997). To properly characterize PDFs, it is necessary to measure their crystallographic orientations optically by using either a universal stage (Emmons 1943) or a spindle stage (Medenbach 1985), or by transmission electron microscopy (see, e.g., Goltrant et al. 1991, Leroux et al. 1994).

The formation mechanisms of these features in naturally shocked quartz might be explained by the pressure dependence of the shear modulus (decreasing linearly with increasing pressure and, for some planes even discontinuously, for a critical pressure of the order of 10 GPa) of quartz for various planes and directions. The Si-O-Si bonds are more easily broken, allowing the corresponding atoms to move towards energetically more favourable positions. This progressive reorganization leads to the formation of a new structure (dense amorphous silica lamellae). The transformation occurs very rapidly, as it is

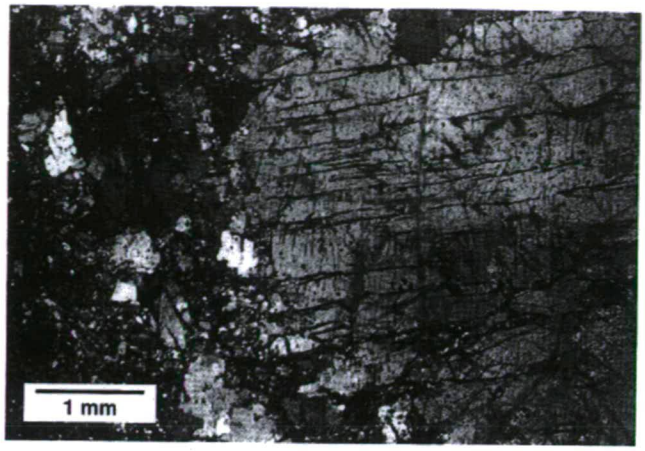


***Fig. 12.*** A quartz grain from metamorphosed orthoquartzite target from the Gardnos impact structure (Norway) exhibits numerous subparallel palanar fractures (longer, dark, subhorizontal lines) and much shorter planar features (short, dark, near-vertical lines). These latter features may be relicts of true PDFs or of Brazil twins parallel to the base (0001) (from French 1998, his Fig. 4.15).

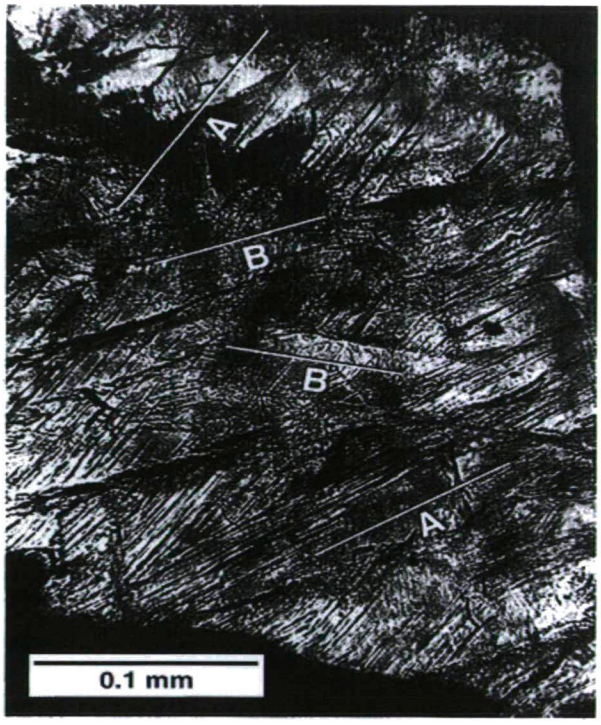


***Fig. 13.*** Multiple sets of PDFs developed in a quartz grain from a shocked granite inclusion in suevite from the Ries Crater (Germany). "A" indicates PDFs parallel to $\{10\bar{1}3\}$ identical $\{01\bar{1}3\}$; "B" indicates PDFs parallel to $\{10\bar{1}1\}$ identical $\{01\bar{1}1\}$. Note the irregular extinction within the quartz grain (from French, 1998; his Fig. 4.16).

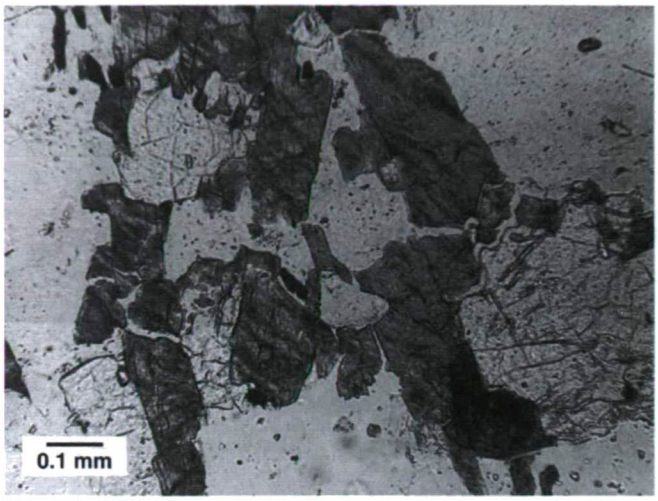


***Fig. 14.*** A biotite gneiss inclusion in suevite breccia, Otting, Ries Crater (Germany) contains diaplectic feldspar glass (maskelynite) (clear, low relief; e.g., upper right) and diaplectic quartz glass (clear, higher relief, e.g., lower right). The associated biotite crystals (dark) have retained their original shape and have remained crystalline and birefrigent, despite the complete transformation of adjacent quartz and plagioclase into glassy phases. Biotite gneiss (from French 1998, his Fig. 4.32).

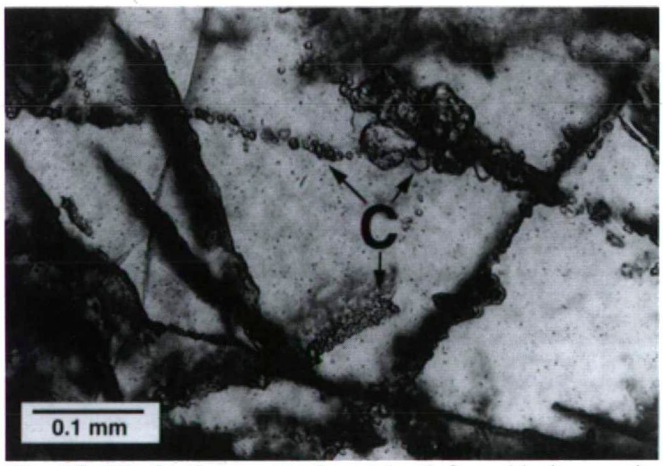


***Fig. 15.*** Diaplectic quartz glass (clear) from biotite granite inclusion in suevite breccia, Aufhausen, Ries Crater (Germany) appears, with strings of small, high-relief crystals of coesite ("C") (from French 1998, his Fig. 4.12).

driven by the front of the shock wave. This explanation predicts that the density of PDFs should markedly increase with shock intensity (Goltrant et al. 1992).

## DIAPLECTIC GLASS, LECHATELIERITE AND HIGH-PRESSURE POLYMORPHS

### *Diaplectic glass*

Diaplectic glass is formed (Tables 1 and 2) at shock pressures in excess of about 35 GPa without melting by solid-state transformation and has been described as a phase intermediate between crystalline and normal glassy phases (Stöffler and Hornemann 1972). It is found at numerous impact craters and shows the original crystal defects, planar features, and absence of flow structures and vesicles. Maskelynite is a diaplectic plagioclase glass formed in a similar way and at similar pressure range as diaplectic quartz glass. Diaplectic glass has a refractive index that is slightly lower than that of synthetic quartz glass (Fig. 14). Other minerals (mafics) tend to oxidize or decompose.

### *Lechatelierite*

At pressures that exceed about 50 GPa, lechatelierite forms by fusion of quartz. In contrast to diaplectic glass, lechatelierite is formed by a liquid state transformation associated with the melting of quartz at higher temperatures (>1700°C) than occur in volcanic processes. This is a good indicator of a meteorite impact origin. Other minerals also melt at sufficiently high temperatures, e.g., feldspar (Stöffler and Langenhorst 1994).

### *High-pressure polymorphs*

The high-pressure $SiO_2$ polymorphs, coesite (Fig. 15) and stishovite, occur as very fine-grained aggregates that are formed by partial transformation of the host quartz during shock metamorphism (Grieve et al. 1996). Under conditions of static equilibrium, where reaction rates are slower and kinetic factors less important, coesite forms from quartz at lower pressures (>2 GPa) than does stishovite (10-15 GPa) (French 1998). The identification of coesite and stishovite at several impact sites in the early 1960s provided one of the earliest criteria for establishing the impact origin of several structures, most notably the Ries crater, Germany (Chao et al. 1960, Shoemaker and Chao 1961), and the Bosumtwi crater (Littler et al. 1961). Impact-derived coesite occurs as very fine-grained, colorless to brownish, polycrystalline aggregates, up to 100-200 μm in size, usually embedded in diaplectic quartz glass, or rarely, in nearly isotropic quartz with abundant planar deformation features and a mean refractive index below 1.48 (Stöffler and Langenhorst 1994) (Fig. 15). Coesite occurs also in metamorphic rocks of ultra-high pressure origin.

Other high-pressure mineral phases include jadeite formed from plagioclase, majorite from pyroxene, and ringwoodite from olivine (Stöffler 1972). Impact derived diamonds (the high-pressure cubic modification of carbon) have also been found at various craters. These diamonds form from carbon in the target rocks, mainly in graphite-bearing (e.g., graphitic gneiss) or coal-bearing rocks (Koeberl et al. 1997b).

### *A new mineralogical indicator of shock metamorphism: zircon*

Zircon is a refractory and weathering-resistant mineral that has been proven useful as an indicator of shock metamorphism in the study of impact structures and formations that are old, deeply eroded, and metamorphically overprinted. Thus, it has advantages compared to quartz or other shock-metamorphosed minerals that have been previously used as impact indicators, but are far less refractory than zircon.

Shock-induced microdeformation in zircon has been described in samples from a variety of impact environments, including material from confirmed impact structures (Åberg and Bollmark (1985), Bohor et al. (1993), Krogh et al. (1984), Wittmann et al. (2006) from the Cretaceous-Tertiary boundary, and from the Upper Eocene impact ejecta layer Bohor et al. (1993), Kamo and Krogh (1995), Glass and Liu

(2001), as well as in experimentally shock-deformed single-crystal zircon (Deutsch and Schärer 1990, Leroux et al. 1999, Gucsik et al. 2002). Two different types of shock deformation have been observed: (i) planar microdeformations and (ii) granular (also called polycrystalline, microcrystalline, *strawberry*) texture. Some effort, especially by transmission electron microscopy (TEM), has been made to determine whether the planar microdeformations discernable at the optical scale in shock-metamorphosed zircon represent *bona fide* planar deformation features (PDFs), well-known from many other shock-metamorphosed rock-forming minerals French (1998), Stöffler and Langenhorst (1994) Grieve et al. (1996), or whether they represent planar fractures or some other type of microdeformation (Reimold et al. 2002). To date, this problem has not been solved. Leroux et al. (1999) established that, on a nanometer scale, amorphous phases in the form of planar lamellae were formed in experimentally shocked zircon (pressure range: 20-40 GPa). However, these authors were not able to confirm that these micro-lamellae, resembling PDFs, indeed corresponded to the optically resolved, several μm wide, planar/subplanar microdeformations.

The granular texture of zircon was first observed by Bohor et al. (1993) in zircon from the Cretaceous/Tertiary distal impact ejecta layer. Since then, it has been observed in zircon from a number of impact structures (Kamo et al. 1996 and references therein), in zircon from a Late Eocene microkrystite layer, and in tektites (Glass and Liu 2001, Deloule et al. 2001). Complete breakdown of zircon to baddeleyite, presumably as a result of high-temperature dissociation, has been identified in Libyan Desert Glass and corroborated the impact origin of these enigmatic glasses Kleinmann (1969).

Leroux et al. (1999) confirmed through their TEM investigations of experimentally shocked zircon that the phase transformation from the zircon structure to a scheelite ($CaWO_4$)-type phase that had been previously observed in shock-metamorphosed zircon by Kusaba et al. (1985) was nearly complete at 60 GPa shock pressure. In the 60 GPa samples of Leroux et al. (1999) shock deformation effects (nanometer-sized PDFs) were observed in a few relict domains consisting of zircon. More recently, new techniques and methodologies such as SEM, CL, micro-Raman and IR have been applied to identify reidite from shocked zircon samples of shock recovery experiments and naturally shock-metamorphosed samples from Ries impact structure (Gucsik et al. 2004).

*Shocked clay minerals*

Clay minerals have been found from different shock metamorphic environments such as Cretaceous/Tertiary Boundary layers (Pollastro and Bohor 1993, Salge et al. 2000), terrestrial impact structures (Dypvik and Ferrell 1998, Krisimäe et al. 2002, Dypvik et al. 2003, Uysal et al. 2003, Horton et al. 2006), and meteorites (Scott and Krott 1998).

In a pioneering study, shocked clay samples from a Barents Sea borehole near the Mjølnir Impact Structure were used to investigate changes in the clay assemblage associated with the submarine impact (Dypvik and Ferrell 1998). They found increased abundance of a smectite, a randomly interstratified smectite-illite with 85% smectite layers, forms the basis for a two-layer oceanic impact clay model that differs from published terrestrial cases. The smectite is assumed to represent seawater-altered impact glass from the ejecta blanket material that was mixed with resuspended shelf sediments by the collision generated waves. The smectite-rich interval is overlained by a coarser unit containing abundant smectite, shocked quartz grains, and anomalous Ir contents at its base. This interval may have originated as a density/turbidity current, generated by the impact and the collapse and erosion of the crater rim.

More recently, clay minerals were described from shocked granitoid basement rocks of Woodleigh impact structure (Australia), which are mainly smectite-rich (>75%) mixed-layer illite-smectite with some discrete illite formed as an alteration-product (replacement) of biotite (Uysal et al. 2003). They concluded that these clay minerals formed by post-shock hydrothermal alteration processes.

**ACKNOWLEDGEMENTS**

As this study was a part of my Ph.D. thesis, I would like to express thank to Profs. Christian Koeberl, Eugen Libowitzky, Uwe Reimold, and Franz Brandstätter supervising my Ph.D. studies at the University of Vienna, Austria.

**REFERENCES**

ÅBERG, G., BOLLMARK, B. (1985): Retention of U and Pb in zircons from shocked granite in the Siljan impact structure, Sweden. Earth and Planetary Science Letters, **74**, 347–49.

BARRAT.A., JAHN, B.M., AMOSSE, J., ROCCHIA, R., KELLER, F., POUPEAU, G.R., DIEMER, E. (1997): Geochemistry and origin of Libyan Desert glasses. Geochimica et Cosmochimica Acta, **61**, 1953–959.

BERAN, A. KOEBERL, C. (1997) Water in tektites and impact glasses by FTIR spectrometry. Meteoritics and Planetary Science, **32**, 211–16.

BIGAZZI, G., DE MICHELE, V. (1996): New fission-track age determination on impact glasses. Meteoritics and Planetary Science, **31**, 234–36.

BLUM, J.D., CHAMBERLAIN, C.P., HINGSTON, M.P, KOEBERL, C., MARIN, L.E., SCHURAYTZ, B.C., SHARPTON, V.L. (1993): Isotopic comparison of K-T boundary impact glass with melt rock from the Chicxulub and Manson impact structures. Nature, **364**, 325–327.

BOHOR, B. F., BETTERTON, W. J., KROGH, T. E. (1993): Impact-shocked zircons: discovery of shock-induced textures reflecting increasing degrees of shock metamorphism. Earth and Planetary Science Letters, **119**, 419–424.

BUNCH, T.E. (1968): Some characteristics of selected minerals from craters. In: French, B.M., Short, N.M. (Eds.), Shock metamorphism of natural materials. Mono Book Corporation, Baltimore, 413–432.

CHAO, E.C.T., SHOEMAKER, E.M., MADSEN, B.M. (1960): First natural occurrence of coesite. Science, **132**, 220–222.

CIPRIANI, C., CORAZZA, M., GIULI, G., CECCHI, V. N., PRATESI, G., ROSSI, P., VITTONE, E. (2000): Ion beam study of a possible extraterrestrial body signature in Lybian desert glass. Nuclear Instruments and Methods in Physical Research B, **170**, 187–192.

DELOULE, E., CHAUSSIDON, M., GLASS, B.P., KOEBERL, C. (2001): U-Pb isotopic study of relict zircon inclusions recovered from Muong Nong-type tektite. Geochimica et Cosmochimica Acta, 65, 1833-1838.

DENCE, M. R. (1972): The nature and significance of terrestrial impact structures. 24th International Geological Congress, Montreal, Canada. Proceedings Section, **15**, 77–89.

DEUTSCH, A. (1998): Examples for terrestrial impact structures. In: MARFUNIN, S.A. (Ed.), Mineral matter in space, mantle, ocean floor, biosphere, environmental management, and jewelry. Springer-Verlag, Berlin, Heidelberg, Advanced Mineralogy, **3**, 119–129.

DEUTSCH, A., SCHARER, U. (1990): Isotope systematics and shock-wave metamorphism: I. U-Pb in zircon, titanite, and monazite, shocked experimentally up to 59 GPa, Geochimica and Cosmochimica Acta, **54**, 3427–3434.

DIEMER, E. (1997): Libyan Desert Glass: an impactite. State of the art in July 1996. In: de Michelle V. (ed.), Silica '96 Proceedings of Meeting on Libyan Desert Glass and related events: Milan, Italy, Pyramids, 29–36.

DIETZ, R.S. (1968): Shatter cones in cryptoexplosion structures. In: FRENCH, B.M., SHORT, N.M. (Eds.), Shock metamorphism of natural materials. Mono Book Corporation, Baltimore, 267–285.

DYPVIK, H., FERREL, R.E. (1998): Clay mineral alteration associated with meteorite impact in the marine environment (Barents Sea). Clay Minerals, **33**, 51–64.

DYPVIK, H., FERREL, R.E., SANDBAKKEN, P.T. (2003): The clay mineralogy of sediments relate to the marine Mjolnir impact crater. Meteoritics and Planetary Science, **38**, 1437–1450.

EL GORESY, A. (1965): Baddeleyite and its significance in impact glasses. Journal of Geophysical Research, **70**, 3453–3456.

EL GORESY, A., FECHTIG, H., OTTEMANN, T. (1968): The opaque minerals in impactite glasses. In: French, B.M., Short, N.M. (Eds.), Shock Metamorphism of Natural Materials, Mono Book Co., Baltimore, Maryland, USA, 531–553.

EMMONS, R.C. (1943): The Universal Stage (With Five Axes of Rotation). Geological Society of America Memoir, **8**, 205.

FRENCH, B.M. (1998): Traces of Catastrophe: A Handbook of Shock-Metamorphic Effects in Terrestrial Meteorite Impact Structures. LPI Contribution No. 954, Lunar and Planetary Institute, Houston, 120.

FRENCH, B.M., SHORT, N. M., (Eds) (1968): Shock metamorphism of natural materials. Mono Book Corporation, Baltimore, 644 pp.

FRENCH, B.M., HARTUNG, J.B., SHORT, N.M., DIETZ, R. S. (1970): Tenoumer crater, Mauritania: Age and petrologic evidence for origin by meteorite impact. Journal of Geophysical Research, **75**, 4396–4406.

FUDALI, R.F., CRESSY, P.J. (1976): Investigation of a new stony meteorite from Mauritania with some additional data on its find site: Aouelloul crater. Earth and Planetary Science Letters, **30**, 262–268.

GASH, P.J.S. (1971): Dynamic mechanism for the formation of shatter cones. Nature, **230**, 32–35.

GAULT, D.E., QUAIDE, W.L., OBERBECK, V.R. (1968): Impact cratering mechanics and structures. In: French, B.M., Short, N.M. (Eds.), Shock Metamorphism of Natural Materials. Mono Book Corporation, Baltimore, 87–99.

GLASS, B.P. (1972): Crystalline inclusions in a Muong Nong-type indochinite. Earth and Planetary Science Letters, **16**, 23–26.

GLASS, B.P., LIU, S. (2001): Discovery of high-pressure $ZrSiO_4$ polymorph in naturally occurring shock-metamorphosed zircons. Geology, **29**, 371–373.

GLASS, B.P., BARLOW, R.A. (1979): Mineral inclusions in Muong Nong-type indochinites: Implications concerning parent material and process of formation. Meteoritics, **14**, 55–67.

GOLTRANT, O., LEROUX, H., DOUKHAN J.-C., CORDIER, P. (1992): Formation mechanism of planar deformation features in naturally shocked quartz. Physics of the Earth Planetary Interiors, **74**, 219–240.

GOLTRANT, O., CORDIER, P., DOUKHAN, J.C. (1991): Planar deformation features in shocked quartz: a transmission electron microscopy investigation. Earth and Planetary Science Letters, **106**, 103–115.

GRIEVE, R.A.F. (1991): Terrestrial impact: The record in the rocks. Meteoritics, **26**, 175–194.

GRIEVE, R.A.F. (1987): Terrestrial impact structures. Annual Reviews of Earth and Planetary Science, **15**, 245–270.

GRIEVE, R.A.F., LANGENHORST, F., STÖFFLER, D. (1996): Shock metamorphism of quartz in nature and experiment: II. Significance in geoscience. Meteoritics and Planetary Science, **31**, 6–35.

GUCSIK, A., KOEBERL, C., BRANDSTATTER, F., LIBOWITZKY, E., REIMOLD, W.U. (2004): Cathodoluminescence, electron microscopy, and Raman spectroscopy of experimentally shock metamorphosed zircon crystals and naturally shocked zircon from the Ries impact crater. In Dypvik, H., Burchell, M., Claeys, PH. (eds.): Cratering in Marine Environments and on Ice, Springer-Verlag, Heidelberg, 281–322.

GUCSIK A., KOEBERL, C., BRANDSTATTER, F., REIMOLD, W.U., LIBOWITZKY, E. (2002): Cathodoluminescence, electron microscopy, and Raman spectroscopy of experimentally shock-metamorphosed zircon. Earth and Planetary Science Letters, **202**, 495–509.

HORN, P., MÜLLER-SOHNIUS, D., SCHAAF, P., KLEINMANN, B., STORZER, D. (1997): Potassium-argon and fission-track dating of Lybian Desert Glass, and strontium and neodymium isotope constraints on its source rocks. In: de MICHELE, V. (Ed.), Proceedings of Meeting on Libyan Desert Glass and related events: Milan, Italy, Pyramids, 59–73.

HORTON, W.J, JR., VANKO, D.A., NAESER, CH.W. (2006): Postimpact hydrothermal conditions at the central uplift, Chesapeake Bay impact structure, Virginia, USA. 38th Lunar and Planetary Science Conference, #1642.

HÖRZ, F. (1982): Ejecta of the Ries crater, Germany. In: SILVER, L. T., SCHULTZ, P. H. (Eds.), Geological implications of impacts of large asteroids and comets on the Earth. Geological Society of America Special Paper, **190**, 39–55.

HÖRZ, F., QUAIDE, W.L. (1973): Debye-Scherrer investigations of experimentally shocked silicates. The Moon, **6**, 45–82.

KAMO, S.L., KROGH, T.E. (1995): Chicxulub crater source for shocked zircon crystals from the Cretaceous-Tertiary boundary layer, Saskatchewan: Evidence from new U-Pb Data. Geology, **23**, 281–284.

KAMO, S.L., REIMOLD, W.U., KROGH, T.E., COLLISTON, W.P. (1996): A 2.023 Ga age for the Vredefort impact event and first report of shock metamorphosed zircons in pseudotachylitic breccias and Granophyre. Earth and Planetary Science Letters, **144**, 369–387.

KIEFFER, S.W., SIMONDS, C.H. (1980): The role of volatiles and lithology in the impact cratering process. Reviews of Geophysics and Space Physics, **18**, 143–181.

KLEINMANN, B. (1969): The breakdown of zircon observed in the Libyan Desert Glass as evidence of its impact origin. Earth and Planetary Science Letters, **5**, 497–501.

KOEBERL, C. (1997): Impact cratering: the mineralogical and geochemical evidence. In: Johnson, K.S., Campbell, J.A. (eds.),

Ames structure in northwest Oklahoma and similar features: origin and petroleum production (1995 symposium). Oklahoma Geological Survey Circular, **100**, 30–54.

KOEBERL, C. (1994): African meteorite impact craters: Characteristics and geological importance. Journal of African Earth Sciences, **18**, 263–295.

KOEBERL, C. (1992a): Water content of glasses from the K/T boundary, Haiti: indicative of impact origin. Geochimica et Cosmochimica Acta, **56**, 4329–332.

KOEBERL, C. (1992b): Geochemistry and origin of Muong Nong-type tektites. Geochimica and Cosmochimica Acta **56**, 1033–1064.

KOEBERL, C., AUER, P. (1991): Geochemistry of impact glass from the Aouelloul crater, Mauritania. 22nd Lunar and Planetary Science Conference, 731–732.

KOEBERL, C., REIMOLD, W.U., SHIREY, S.B. (1998): The Aouelloul crater, Mauritania: On the problem of confirming the impact origin of a small crater. Meteoritics and Planetary Science, **33**, 513–517.

KOEBERL, C., BOTTOMLEY, R., GLASS B.P., STORZER, D. (1997a): Geochemistry and age of Ivory Coast tektites and microtektites. Geochimica et Cosmochimica Acta, **61**, 1745–1772.

KOEBERL, C., MASAITIS, V.L., SHAFRANOVSKY, G.I., GILMOUR, I., LANGENHORST, F., SCHRAUDER, M. (1997b): Diamonds from the Popigai impact structure, Russia. Geology, **25**, 967–970.

KUSABA K., SYONO Y., KIKUCHI M., FUKUOKA K. (1985) Shock behaviour of zircon: phase transition to scheelite structure and decomposition. Earth and Planetary Science Letters, **72**, 433–439.

KRISIMAE, K., SUUROJA, S., KIRS, J., KARKI, A., POLIKARPUS, M., PUURA, V., SUUROJA, K. (2002): Hornblende alteration and fluid inclusions in Kardla impact crater, Estonia: evidence for impact-induced hydrothermal activity. Meteoritics and Planetary Science, **37**, 449–457.

KROGH, T.E., DAVIS, W.D., CORFU, F. (1984): Precise U-Pb zircon and baddeleyite ages for the Sudbury area. In: Pye, E.G., Naldrett, P.E., Giblin, P.E. (eds.), The Geology and Ontario Geolological Survey Special Paper, **1**, 431–446.

LEROUX H., REIMOLD W.U., KOEBERL C., HORNEMANN U., DOUKHAN J.-C. 1999. Experimental shock deformation in zircon: a transmission electron microscopic study. Earth and Planetary Science Letters, **169**, 291–301.

LEROUX, H., REIMOLD, W.U., DOUKHAN, J.C. (1994): A T.E.M. investigation of shock metamorphism in quartz from the Vredefort dome, South Africa. Tectonophysics, **230**, 223–239.

LITTLER, J., FAHEY, J.J., DIETZ, R.S., CHAO, E.C.T. (1961): Coesite from the Lake Bosumtwi crater, Ashanti, Ghana. Geological Society of America Special Paper, **68**, 218.

MARTINEZ, I., AGRINIER, P. (1998): Meteorite impact craters on Earth: major shock induced effects in rocks and minerals. Earth and Planetary Sciences, **327**, 75–86.

MARTINEZ, I., DEUTSCH, A., SCHARER, U., ILDEFONSE, P., GUYOT, F., AGRINIER, P. (1995): Shock recovery experiments on dolomite and thermodynamical calculations of impact induced decarbonation. Journal of Geophysical Research, **100**, 15,465–15,476.

MCHONE, J.F., KILLGORE, M., KUDRYAVTSEV, A. (2000): Cristobalite inclusions in Libyan Desert Glass: confirmation using Raman spectroscopy. 31st Lunar and Planetary Science Conference, #1877.

MEDENBACH, O. (1985): A new microrefractometer spindle stage and its application. Fortschritte der Mineralogie, **63**, 111–133.

MEISEL, T., KRAHENBÜHL, U., NAZAROV, M.A. (1995): Combined osmium and strontium isotopic study of the Cretaceous-Tertiary boundary at Sumbar, Turkmenistan: A test for an impact vs. volcanic hypothesis. Geology, **23**, 313–316.

MELOSH, H.J. (1992): Impact crater geology. In: Nierenberg, W.A. (Ed.), Encyclopedia of Earth System Science 2. Academic Press, San Diego, 591–605.

MELOSH, H.J. (1989): Impact Cratering: A geologic process. Oxford University Press, New York, 245.

MONTANARI, A., KOEBERL, C. (2000): Impact Stratigraphy: The Italian Record. Lecture Notes in Earth Sciences 93, Springer, Heidelberg, 364.

MURALI, A.V., ZOLENSKY, M.E., UNDEWOOD, J.R., JR., GIEGENGACK, R.F. (1997): Chondritic debris in Libyan Desert Glass. In: de Michelle V. (Ed.), Proceedings of Meeting on Libyan Desert Glass and related events: Milan, Italy, Pyramids, 133–142.

PIAZENZA, B. (1997): Evidence of granular structure of Libyan Desert Silica Glass by SEM cathodoluminescence. In: de Michelle V. (Ed.), Proceedings of Meeting on Libyan Desert Glass and related events: Milan, Italy, Pyramids, 85–90.

POLLASTRO, R. M., BOHOR, B.F. (1993): Origin and clay-mineral genesis of the Cretaceous/Tertiary Boundary Unit, Western Interior of North America. Clays and Clay Minerals, **41**, 7–25.

REIMOLD, W.U. (1995): Pseudotachylite in impact structures – generation by friction melting and shock brecciation?: A review and discussion. Earth Science Reviews, **39**, 247–265.

REIMOLD, W.U., LEROUX, H., GIBSON, R.L. (2002): Shocked and thermally metamorphosed zircon from the Vredefort impact structure, South Africa: A transmission electron microscopic study. European Journal of Mineralogy, **14**, 859–868.

ROCCHIA, R., ROBIN, E., FRÖCHLICH F., AMOSE, J., BARRAT, J-A., MEON, H., FROGET, L., DIEMER, E., (1997): The impact origin of Libyan Desert Glass. In: de Michele, V. (Ed.), Proceedings of Meeting on Libyan Desert Glass and related events: Milan, Italy, Pyramids, 143–149.

RODDY, D.J., PEPIN, R.O., MERRILL, R.B., (Eds.) (1977): Impact and explosion cratering. Pergamon Press, New York, 1301.

ROBERTSON, P.B., DENCE, M.R., VOS, M.A. (1968) : Deformation in rock-forming minerals from Canadian craters. In: French, B.M., Short, N.M., (Eds.) Shock metamorphism of natural materials. Mono Book Corporation, Baltimore, 433–452.

SALGE, T., TAGLE, R., CLAEYS, P. (2000): Accretionary lapilli from the K/T Boundary site of Guayal, Mexico: Preliminary insights of expansion plume formation. 63rd Annual Meteoritical Society Meeting, #5124.

SCOTT, E.R.D., KROT, A.N. (1998): Formation of pre-impact interstitial carbonates in the ALH84001 Martian meteorite. 61st Annual Meteoritical Society Meeting, #5296.

SHAGY, A., RECHES, Z., FINEBERG, J., 2002. Dynamic fracture by large extraterrestrial impacts as the origin of shatter cones. Nature, **418**, 310–313.

SHARPTON, V.L., GRIEVE, R.A.F. (1990): Meteorite impact, cryptoexplosion, and shock metamorphism; A perspective on the evidence at the K/T boundary. Geological Society of America Special Paper, **247**, 301–318.

SHOEMAKER, E.M., CHAO, E.C.T. (1961): New evidence for the impact origin of the Ries Basin, Bavaria, Germany. Journal of Geophysical Research, **66**, 3371–3378.

STORZER, D., KOEBERL, C. (1991): Uranium and zirconium enrichments in Libyan Desert Glass. Zircon, baddeleyite and high-temperature history of the glass. 22nd Lunar and Planetary Science Conference, 1345–1346.

STORZER, D., WAGNER, G.A. (1977): Fission track dating of meteorite impacts. Meteoritics, **12**, 368.

STÖFFLER, D. (1974): Deformation and transformation of rock-forming minerals by natural and experimental processes: II. Physical properties of shocked minerals. Fortschritte der Mineralogie, **51**, 256–289.

STÖFFLER, D. (1972): Deformation and transformation of rock-forming minerals by natural and experimental shock processes: I. Behaviour of minerals under shock compression. Fortschritte der Mineralogie, **49**, 50–113.

STÖFFLER, D., GRIEVE, R.A.F. (1994): Classification and nomenclature of impact metamorphic rocks. 25th Lunar and Planetary Science Conference, 1347–1348.

STÖFFLER, D., LANGENHORST, F. (1994): Shock metamorphism of quartz in nature and experiment: I. Basic observation and theory. Meteoritics, **29**, 155–181.

STÖFFLER, D., HORNEMANN, U. (1972): Quartz and feldspar glasses produced by natural and experimental shock. Meteoritics, **7**, 371–394.

UYSAL, I.T., GOLDING, S.D., GLIKSON, A.Y., MORY, A.J., GLIKSON, M. (2003): K-Ar evidence from illitic clays of a Late Devonian age of the 120 km diameter Woodleigh impact structure, Southern Carnarvon Basin, Western Australia. Earth and Planetary Science Letters, **192**, 281–289.

WITTMANN, A., KENKMANN, T., SCHMITT, R.T. STÖFFLER, D. (2006): Shock metamorphosed zircon in terrestrial impact craters. Meteoritics and Planetary Sciences, **40**, 1–16.

*Received: June 13, 2008; accepted: December 9, 2008*